



# Analysis of Dry Sliding Wear Behavior of Polyester Filled with Walnut Shell Powder Using Response Surface Method and Neural Networks

Priyabrat Pradhan and Alok Satapathy

Submitted: 27 November 2020 / Revised: 28 March 2021 / Accepted: 5 April 2021 / Published online: 28 April 2021

This paper reports on the critical analysis of the dry sliding wear characteristics of polyester-based composites through systematic experimentation integrated with artificial neural networks (ANN) and response surface methodology (RSM). In this study, composites are fabricated with unsaturated polyester resin as the matrix material and micro-sized walnut shell powder (WSP) as the particulate filler. Such composites with different filler concentrations have been prepared by simple hand layup technique. The composite characterizations regarding density, porosity and tensile strength are made and validated with the results obtained from a numerical tool Digimat-FE. Further, wear trials are conducted using a standard pin-on-disk machine according to design of experiment based on response surface methodology (RSM). The data obtained from the experiments are considered to train and test an ANN model, which prognosticates the impact of various control factors on wear behavior of the composites. Among all the factors considered for analysis, sliding velocity, filler content, and normal load are found to be the significant factors in that sequence affecting the wear rate of the composites.

**Keywords** artificial neural networks, polyester, response surface methodology, sliding wear analysis, walnut shell powder

## 1. Introduction

In the last few decades, research focus has been expedited towards polymers and their composites from conventional monolithic materials due to their growing tribological applications such as in rollers, clutches, brakes and gears due to high strength, relatively better wear resistance, and low density (Ref 1). These composites are now replacing traditional metal alloys in aerospace, defense, and sporting industry. As polymer composites are lighter in weight, these materials are quiet suitable for weight sensitive uses. But sometimes due to high cost, use of polymer composites is restricted in the commercial applications. So the cost of these components could be brought down by the reinforcement of cheaper materials such as agro waste lightweight fillers. The available literature reveals that different types of fillers have been used as reinforcement in polymer composite (Ref 2). The use of fillers in polymer composites primarily serves two purposes; first improves mechanical, tribological, and thermal properties; second decreases cost of the components (Ref 1). Fillers are mainly

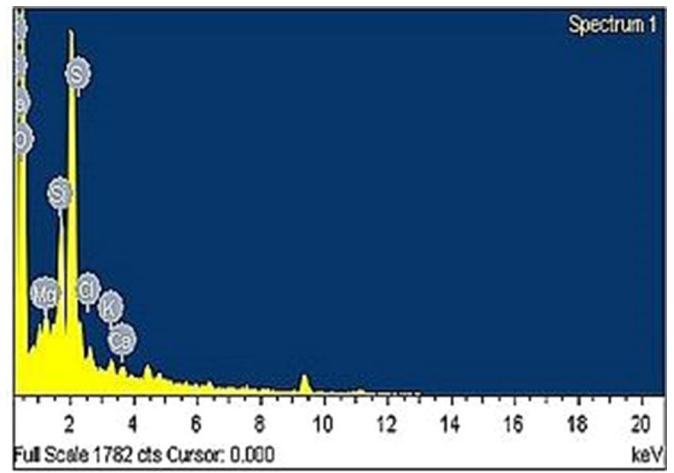
classified into three categories (a) hard fillers (ceramics, metals and minerals), (b) glass fillers, and (c) natural fillers (Teak wood dust, pine wood dust, rice husk, coconut shell dust, palm kernel dust, etc.) (Ref 3). Ceramics and metals are known as hard particulates which are used to increase mechanical and wear resistance of the polymers even up to three order magnitude. Polymer composites with metallic fillers have several industrial applications such as heater, electrode, and components, which require thermal durability at high temperatures. However, due to growing demand of lightweight components, use of plant-based organic fillers in polymer composites is increasing day by day, which is very helpful in cost reduction and stiffness improvement (Ref 4). Addition of coconut shell dust increases bulk hardness of low-density polythene which can be used in automobile interior applications (Ref 5). Asabe (Ref 6) found that thermal stability of PVC which is about 103 °C enhances up to 370 °C due to inclusion of banana stem particulates. Pradhan et al. (Ref 7) recently reported that thermal conductivity of polyester composites significantly affected due to addition of walnut shell powder. Particulate filling not only affects the mechanical and thermal behavior but also significantly improves tribological properties of the composites. Pradhan et al. (Ref 8) observed that abrasive wear losses of epoxy composites have been minimized with 20 wt.% of lantana-camara filler. Aireddy and Mishra (Ref 9) investigated the effects of coir dust concentration on the erosion wear behavior of epoxy composites and found that the erosion resistance of the epoxy resin is improved with increasing volume fraction of filler. Though several number of natural fibers and particulates have been explored, use of walnut shell powder as a filler in polymeric matrices has not been researched adequately. Walnut is a fruit that grows in the trees of genus juglans, and its shell is 67% of the total weight of the walnut kernel. It has been estimated that around 1.5 million tons of shells generate per year all over the world. Its shell, generally dark brown in color and is mostly a waste material with hardly

This invited article is part of a special topical focus in the *Journal of Materials Engineering and Performance* on Surface Engineering. The issue was organized by Dr. M.K. Banerjee, Malaviya National Institute of Technology, Jaipur.

**Priyabrat Pradhan and Alok Satapathy**, National Institute of Technology Rourkela, Rourkela, Odisha, India. Contact e-mail: pbpradhan.26@gmail.com.

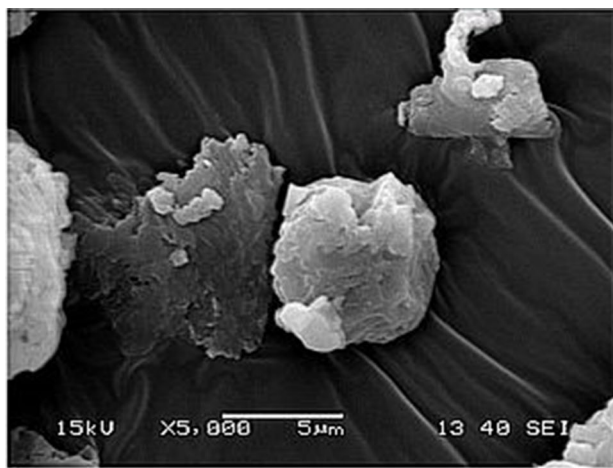


(a)

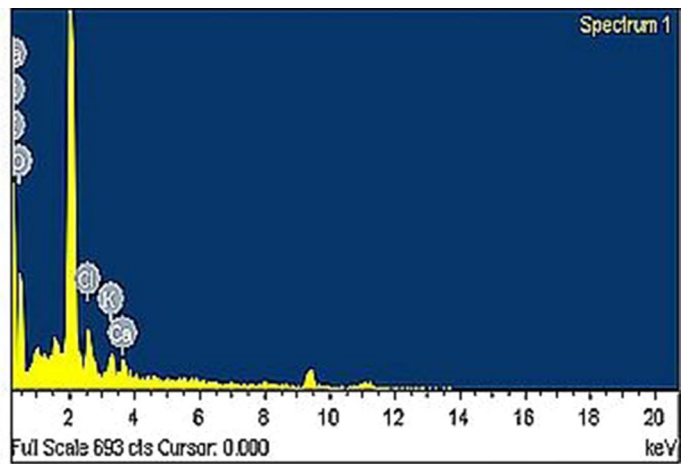


(b)

**Fig. 1** (a) SEM (b) EDS of unsaturated polyester resin

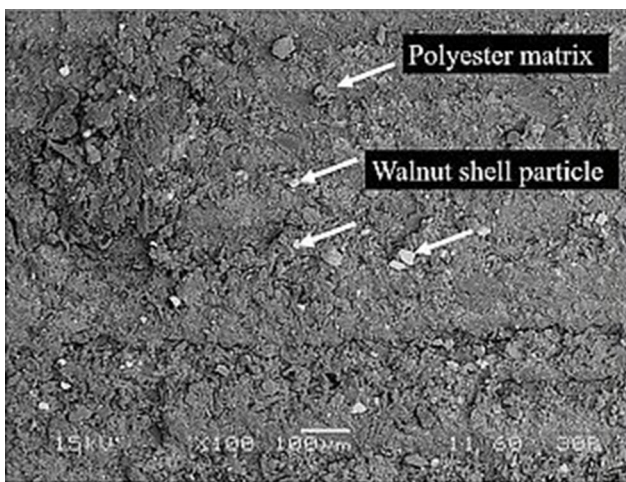


(a)

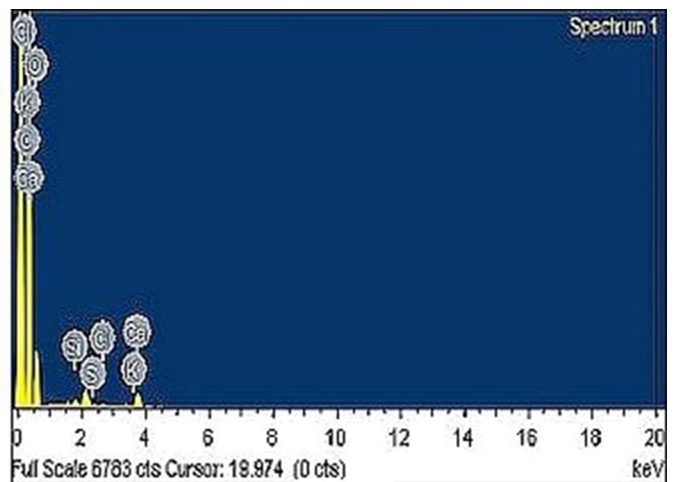


(b)

**Fig. 2** (a) SEM image (b) EDS of walnut shell powder



(a)



(b)

**Fig. 3** (a) SEM (b) EDS of WSP-polyester composite

any significant utilization (Ref 10). As of now, walnut shell powder finds its applications in cosmetics, herbal products, polishing soft metals, glass, wood, plastics and stone (Ref 11). However, walnut shell powder (WSP) is earlier used as filler material in several polymers composites (Ref 12-14), but there is hardly any report on the parametric analysis of sliding wear behavior under different test conditions.

The quality of composites should be analyzed properly because some key parameters like curing temperature and manufacturing speed affect the manufacturing process of material. So the properties of the composite needs to be investigated for special engineering applications (Ref 15). Complex properties like fatigue, wear, modulus, strength and failure strain are to be correlated to understand the interaction

**Table 1 Control factors and their levels for sliding wear test**

Control factors	Level			Units
	I	II	III	
Sliding velocity, $V_s$	100	300	500	cm/s
Sliding distance, $D$	500	1500	2500	m
Normal load, $F_n$	5	10	15	N
Filler content, $f$	4	8	12	wt.%

between them. These relations can be established by a mathematical tool derived from experimental data, which reduces the experimental works required for new test domain. Because of this, ANNs (artificial neural networks) have been introduced to polymer composites to find the complex nonlinear relationship between the properties without any prior assumption (Ref 16). The preliminary investigation of tribological properties using ANN was carried out by Jones et al. on metals (Ref 17). Satyanarayana also evaluated abrasive wear behavior of red mud particle-reinforced aluminum composites by ANN and regression modelling (Ref 18). Recently, in 2015, Padhi et al. performed ANN studies for the prediction of sliding wear behavior of GF/PP composites filled with blast furnace slag (Ref 17).

Against this background, the present study is aimed to foresee the effects of walnut shell powder on the dry sliding wear resistance of polyester resin. This work critically examines the sliding wear characteristics of polyester composites filled with walnut shell powder in different proportions using response surface methodology and artificial neural networks.

## 2. Experimental Details

### 2.1 Matrix and Filler Material

In the present investigation, unsaturated isophthalic polyester resin (density 1.37 g/cm<sup>3</sup>, elastic modulus 1.13 GPa) is

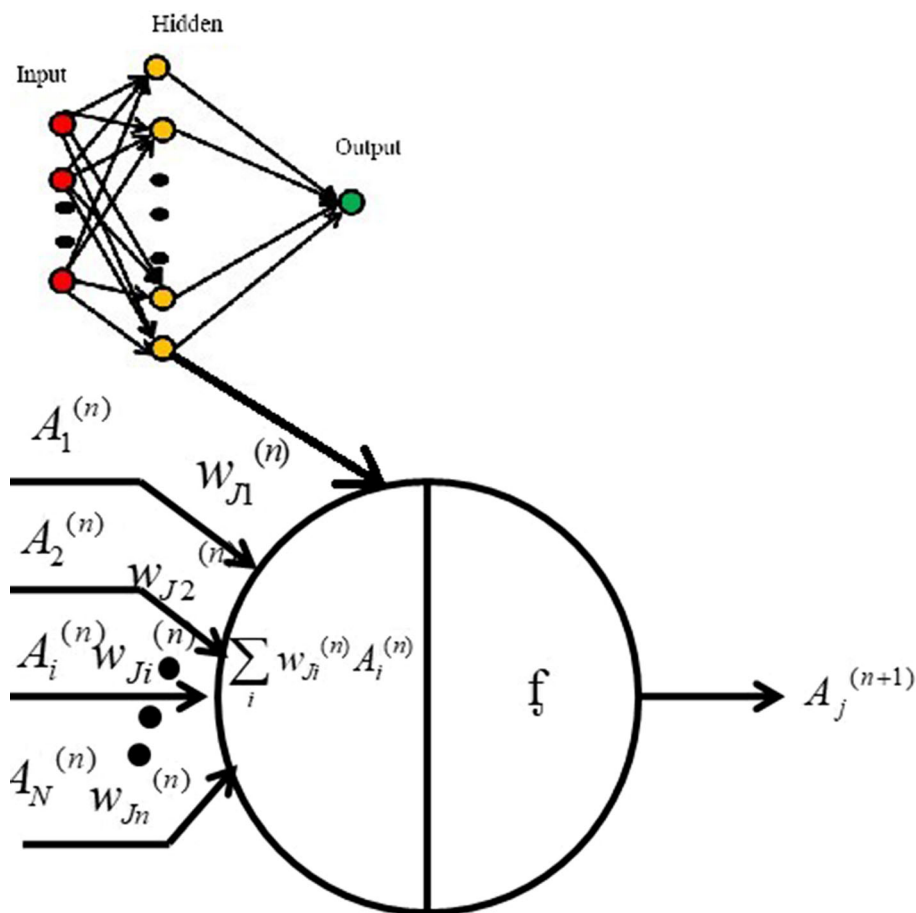
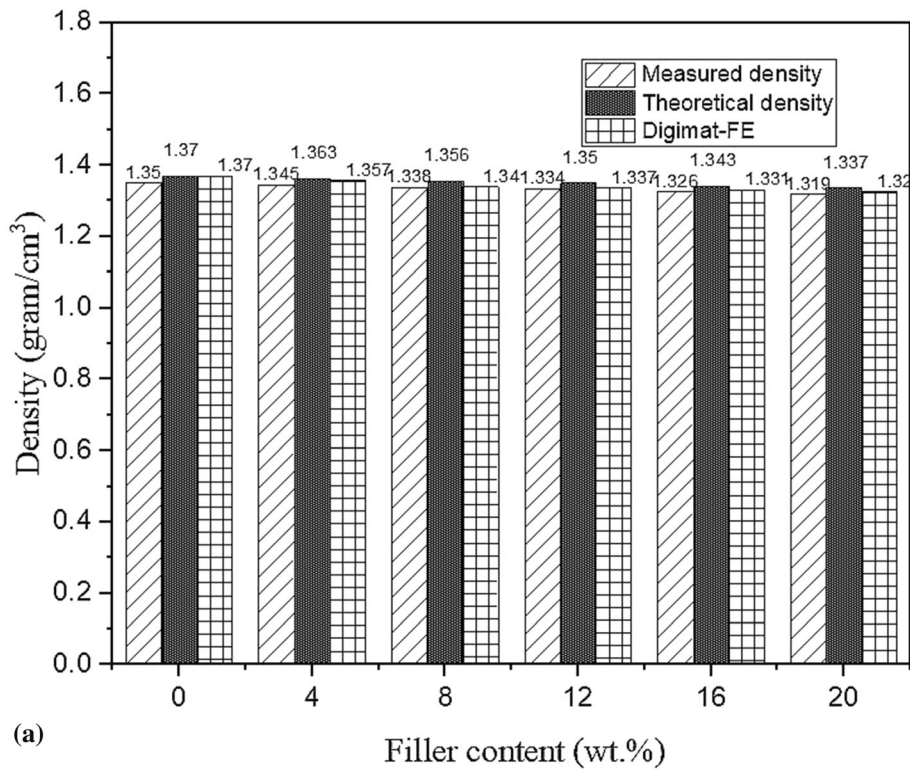
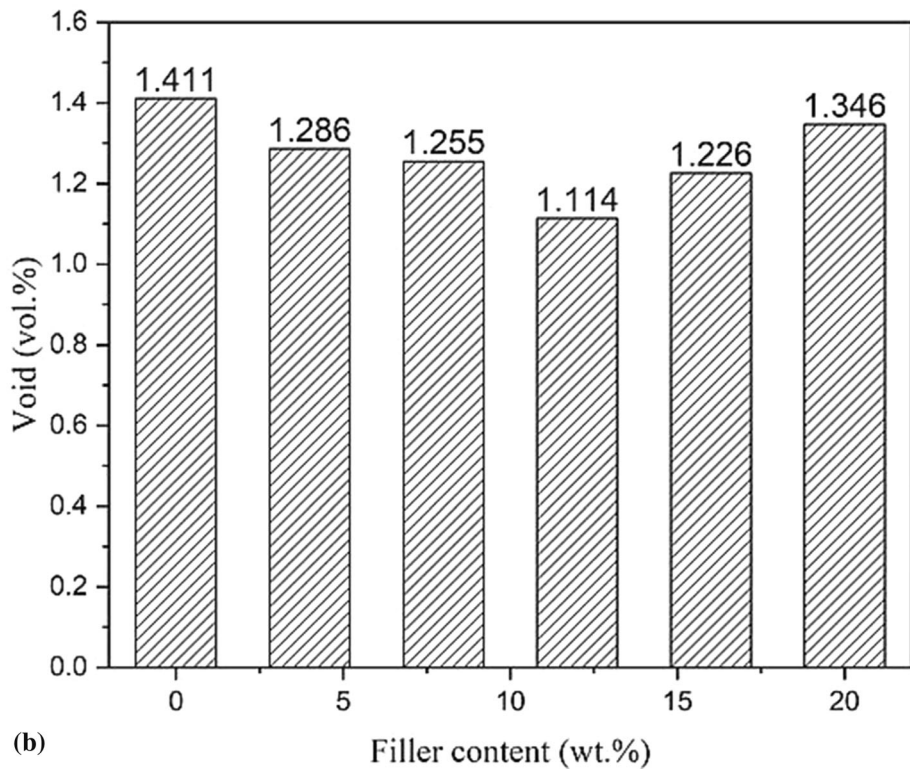


**Fig. 4** Schematic diagram for relation between input and output vector of a single neuron



(a)



(b)

**Figure 5** (a) Measured and theoretical density of the WSP-polyester composite. (b) volume fraction voids (%) for the WSP-polyester composite. (c) Random distributions of fillers and voids for WSP-polyester composites in three different planes

used as matrix material. The polyester resin along its accelerator (cobalt naphenate) and hardener (methyl ethyl ketone peroxide) is supplied by Testing Instrument Manufacturer, Kolkata. The SEM and energy-dispersive x-ray spectroscopy

(EDS) of neat polyester resin is shown in Fig. 1(a) and (b) respectively. The elemental analysis of polyester resin by energy-dispersive x-ray spectroscopy (EDS) reveals that it primarily contains carbon (50.12%), oxygen (37.34%), mag-

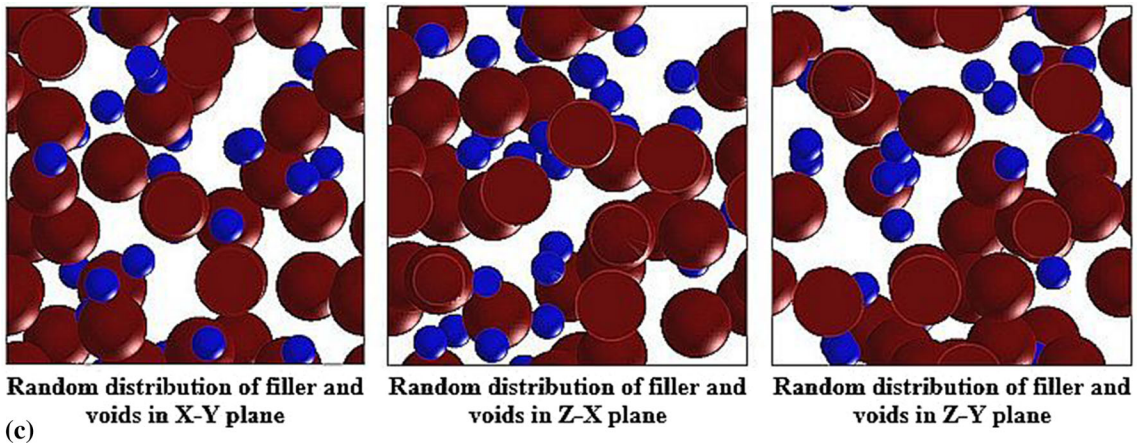


Figure 5 continued

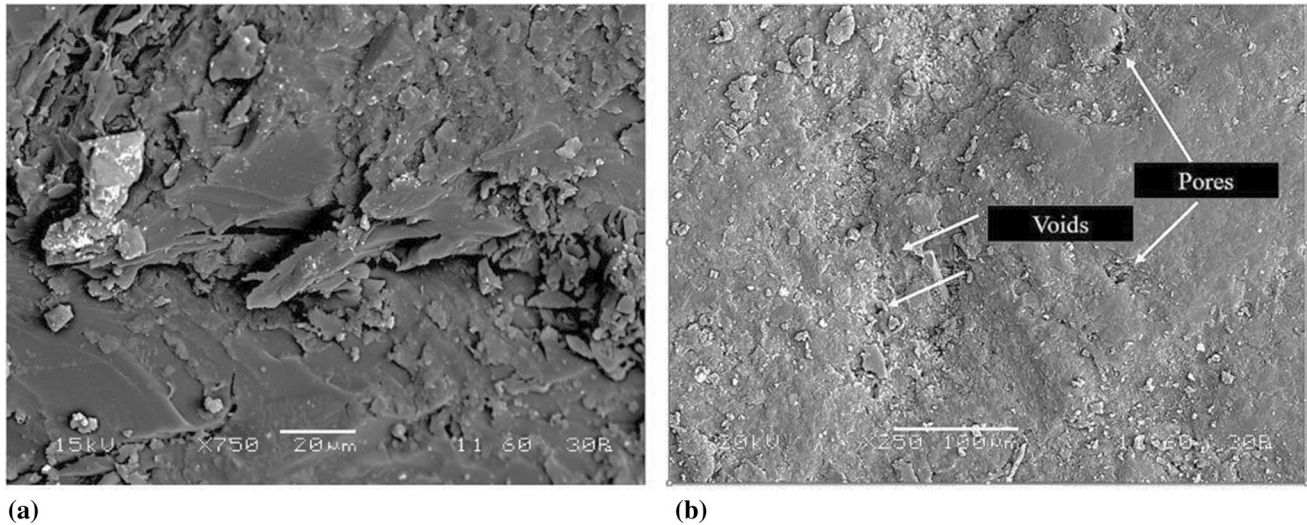


Fig. 6 SEM image of (a) fracture surface of WSP–polyester composite with 12 wt. filler content after tensile test (b) pores and voids present on the surface of composite

nesium (0.21%), silicon (0.97%), sulfur (0.01%), chlorine (0.40%), potassium (0.41%), and calcium (0.46%).

The shells are removed from walnut kernel and washed in acetone to remove surface impurities. These walnut shells are grounded into powder form in a ball mill as a result of which uniform and very small particles are obtained as shown in Fig. 2(a). The particles are then passed through a sieve shaker to obtain an average particle size of 100 μm. The powder is dried in an oven for 48 hours at 100 °C to remove moisture content. It can be observed from the EDS analysis as shown in Fig. 2(b) that the main constituents of walnut shell are carbon (71.01%), oxygen (22.56%), chlorine (2.74%), potassium (2.38%), and calcium (1.31%). The high amount of carbon may be attributed to presence of lignin in the walnut shell powder (Ref 19).

## 2.2 Composite Fabrication

The low-temperature polyester resin is mixed with corresponding accelerator and hardener at a ratio 10:3:3 by weight as recommended. Then 0-20 wt.% walnut shell powder is added to

this homogeneous solution of polyester resin. The amount of filler in the matrix is kept at maximum 20 wt.% as beyond that composite making is not possible because of improper and incomplete wetting. Due to this WSP filler concentration is restricted to 20 wt.% for the present investigation. The prepared dough is then smoothly dented in to wax coated glass tube to obtain cylindrical composite samples of diameter 10 mm and length 120 mm. The mixture of filler and resin is left in the glass molds for 24 hours for curing after which castings are removed by breaking the glass tubes. A typical SEM image of WSP–polyester composites is shown in Fig. 3(a). The size of samples considered for tensile test is 150 mm × 10 mm × 3 mm as per standard ASTM D 3039-76.

## 2.3 Density and Void Fraction

The theoretical density ( $\rho_{act}$ ) and volume fraction of void ( $V_v$ ) of the composites is measured by the Agarwal and Broutman equation (Ref 20). The actual density of the composites is evaluated by Archimedes principle. The theoretical density is also predicted by Digimat-FE software.

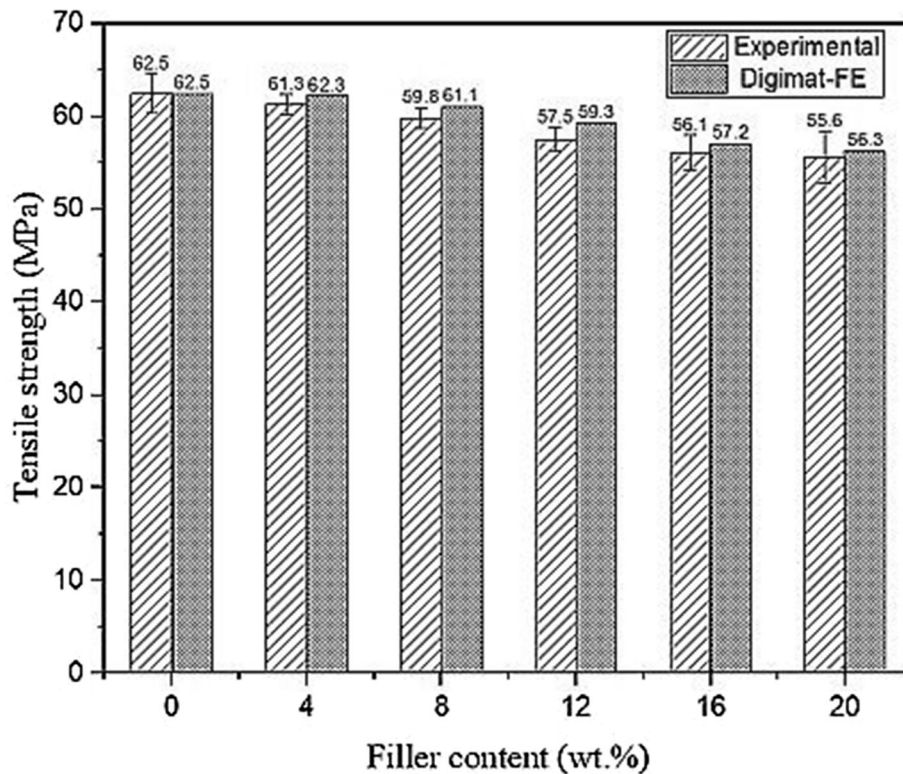


Fig. 7 Comparison between of Digimat-FE predicted and experimental tensile strength of WSP–polyester composites

## 2.4 Tensile Test

The tensile test of the samples is conducted by Universal testing machine (UTM) Instron 1195 with crosshead speed as 10 mm/min. The tensile strength of composites is also calculated by Digimat-FE software and validated with experimental results.

## 2.5 Dry Sliding Wear Test

Dry sliding wear tests are carried out on the WSP–polyester composites in a pin-on-disk test rig as per ASTM G99 standard. The tests are performed on a counterbody of hardened ground steel disk covered with sand paper. When normal load is applied on the composite pin, it is pressed against the rotating disk. Due to which wear is generated at the contact surface between pin and disk. The wear tests are conducted under different parameters as shown in Table 1. An electronic weighing balancing machine is used to weight the samples with an accuracy of  $\pm 0.1$  mg. The disagreement between initial and final measurement of weight of the specimen is the mass loss during the wear test. The volume of material removed per unit load per unit sliding distance is termed as the specific wear rate (SWR) and is expressed as follows:

$$W_s = \frac{\Delta m}{(\rho t V_s F_n)} \quad (\text{Eq 1})$$

where  $\Delta m$  is the mass loss of the composite in the test duration (g),  $\rho$  is the density of the composite ( $\text{g}/\text{mm}^3$ ),  $t$  is the test duration (s),  $V_s$  is the sliding velocity (cm/s), and  $F_n$  is the average normal load (Newton).

## 2.6 Response Surface Methodology (RSM).

In the present study, four major input parameters such as sliding velocity ( $V_s$ ), sliding distance ( $D$ ), normal load ( $F_n$ ) and filler content ( $f$ ) have been considered as response variables each with three levels which influence the specific wear rate of the WSP–polyester composites during the dry sliding wear test. To analyze the impact of these control factors (input) on the wear response (output) large numbers of tests need to be conducted, which is a very laborious task. However, the numbers of experiments could be reduced to great extent by adopting a suitable design of experiment (DoE) approach. So, in this analysis, DoE is carried out by face-centered central composite design (FCCCD) of response surface methodology (RSM). FCCCD is basically an extension of the central composite design (CCD) where axial distance is taken as 1. The response surface methodology (RSM) is used to show the relation between control factors and quality characteristics to reach either maximization or minimization of the out puts. In RSM, the correlation between response  $X$  and a set of independent variable ( $y_1, y_2 \dots y_n$ ) is approximated by a second-order model in the following form

$$x = a_0 + \sum_{i=1}^n a_i y_i + \sum_{i=1}^n a_{ii} y_{ii}^2 + \sum_{i=1}^n a_{ij} y_{ij} + \alpha \quad (\text{Eq 2})$$

where  $\alpha$  is the error or noise observed in the response  $x$ , ( $x - \alpha$ ) is the expected response and values are the regression coefficients to be evaluated (Ref 21).

## 2.7 Modelling with Artificial Neural Networks (ANN)

The neural network concept in the past is used by several researchers in the field of function approximation to generate

the predicted performance output based on the input database. The artificial neural network has been successfully implemented to predict wear dependent statistical parameters (Ref 22, 23). Some major types of neural networks are modular neural networks, feedforward/artificial neural network, radial basis function neural network, kohonen self-organizing neural network, recurrent neural network, convolutional neural network (Ref 15). In this investigation, feedforward/artificial neural network has been used for training and prediction. An ANN model is constructed and trained with statistical data obtained from the experiments. This trained network could be used to predict specific wear rate of any composites. The network is mainly divided into three layers such as input, hidden and output layer. During the training and testing protocol, the generated output is matched with the desired result and the error is returned to hidden layers to enrich the prediction. Figure 4 presents schematic diagram of an ANN configuration. Figure 4 shows that each layer in the network consists several number of neural elements. The network function largely depends upon the connection between these elements. If a single unit of element is considered as shown in Fig. 4, the relation between the input vector  $X_j^{(n)}$  and output vector of the element  $X_j^{(n+1)}$  may be represented as

$$X_j^{(n+1)} = F\left(\sum_i w_{ji}^{(n)} X_j^{(n)}\right) \quad (\text{Eq 3})$$

where the nonlinear sigmoid function

$$F(x) = \frac{1}{1 + e^{-x}} \quad (\text{Eq 4})$$

$X_j^{(n+1)}$  output of unit  $j$  in the  $n$ th layer  $w_{ji}^{(n)}$  weight from unit  $i$  in  $n$ th layer to unit  $j$  in  $(n + 1)$ th layer.

An input vector is assigned to the units of the input layer. The units in the hidden layer evaluate weighted sum of the inputs and produce result of a nonlinear function to the sum. The learning procedure depends on a gradient search with errors between the predicted and desired values:

$$E = \frac{1}{2} \sum_{p=1}^P (d_p - O_p) \quad (\text{Eq 5})$$

where  $E$  total sum of squared error,  $d_p$  target output for  $p$ th pattern,  $O_p$  actual output

This error could be minimized by changing weights using the following equation

$$\Delta W_{ji}^{(n)} = -\eta \frac{\partial E}{\partial W_{ji}^{(n)}} \quad (\text{Eq 6})$$

where  $\eta$  = learning rate.

During preparing a network, information is supplied to ANN many number of times, which is termed as cycle. After each cycle, the error is estimated to improve the quality of the network.

### 3. Results and Discussion

#### 3.1 Density and Void Fraction

The actual density of the WSP–polyester composites is determined by Archimedes' principle whereas the theoretical

density, voids and pores present in the composites are calculated from the Agarwal and Broutman equation (Ref 20). As the pores and voids alter the mechanical and wear properties of the composites, the efficiency of the composites in real working condition could be improved by proper knowledge about them. The actual density, theoretical density and volume fraction of voids of the WSP–polyester composites with different filler loading are presented in Fig. 5(a) and (b) respectively. The density of the composites is also predicted by the Digimat-FE and validated with the experimental results. The Digimat-FE value seems to be in good concurrence with experimental results. Figure 5(a) shows that the density of the composites with 0 w.% filler content is about 1.35 g/cm<sup>3</sup>, which decreases with the addition of walnut shell particles. The abatement of the density of the composite takes place due to the inclusion of relatively low density (1.22 g/cm<sup>3</sup>) WSP filler particles. The random distribution of particles and voids in the WSP–polyester composites is defined by custom phase generation sequence. In this section, the different inclusion phases are identified sequentially in the composites. The periodic geometry of the RVE of the WSP–polyester composites in the X-Y, Z-X, and Z-Y plane is presented in Fig. 5(c). It can be observed from the figure that WSP particles are well distributed throughout the composites whereas maximum voids are present in the middle part of the composites. During fabrication of the composites, the moisture present in the walnut shell powder generates voids in the form of air bubble. But from the surface of the composites, the air is released to the atmosphere, but it is entrapped at the middle portion of the composite. Due to this, maximum voids are present at the center of the composite. The voids present in the composites can be observed clearly in SEM image given in Fig. 6(b).

#### 3.2 Tensile Test

The tensile test of WSP–polyester composites is conducted using an Universal testing machine (UTM) Instron 1195 and the result are shown in Fig. 7. It could be observed from Fig. 7 that tensile strength of neat polyester is about 62.5 MPa, which reduces to 55.6 MPa with the addition of 20 wt.% of WSP filler content. The walnut shell particles consist of lower amount of hygroscopic elements such as cellulose/hemicelluloses and high amount of lignin (Ref 24). Lignin is the major element which significantly reduces the tensile strength (Ref 25). With the addition of walnut shell particles, the lignin percentage increases leads to reduction in the tensile strength of the composites. FE analysis is also used to determine the tensile behavior of WSP–polyester composites with the help of micro-scale Representative Volume Element (RVE). As shown in Fig. 18(h), the shape of walnut shell particle is nearly spherical, due to which RVE with spherical inclusions is considered for FE analysis. The tensile strength predicted by Digimat FE is validated with the experimental result. After generating RVE, meshing is carried out with the help built-in-mesh. Though two types of meshing are available such as conforming mesh and voxel mesh, conforming mesh is used in this analysis. The mechanical loading is applied to the meshed RVE to simulate different types of macroscopic strain fields. The comparison between predicted and experimental values of tensile strength for WSP–polyester composite is shown in Fig. 7. Also, the RVE of WSP–polyester composites with different filler loading along with stress distribution is presented in Fig. 8. The stress distribution in the RVE at the microstructural level is analyzed

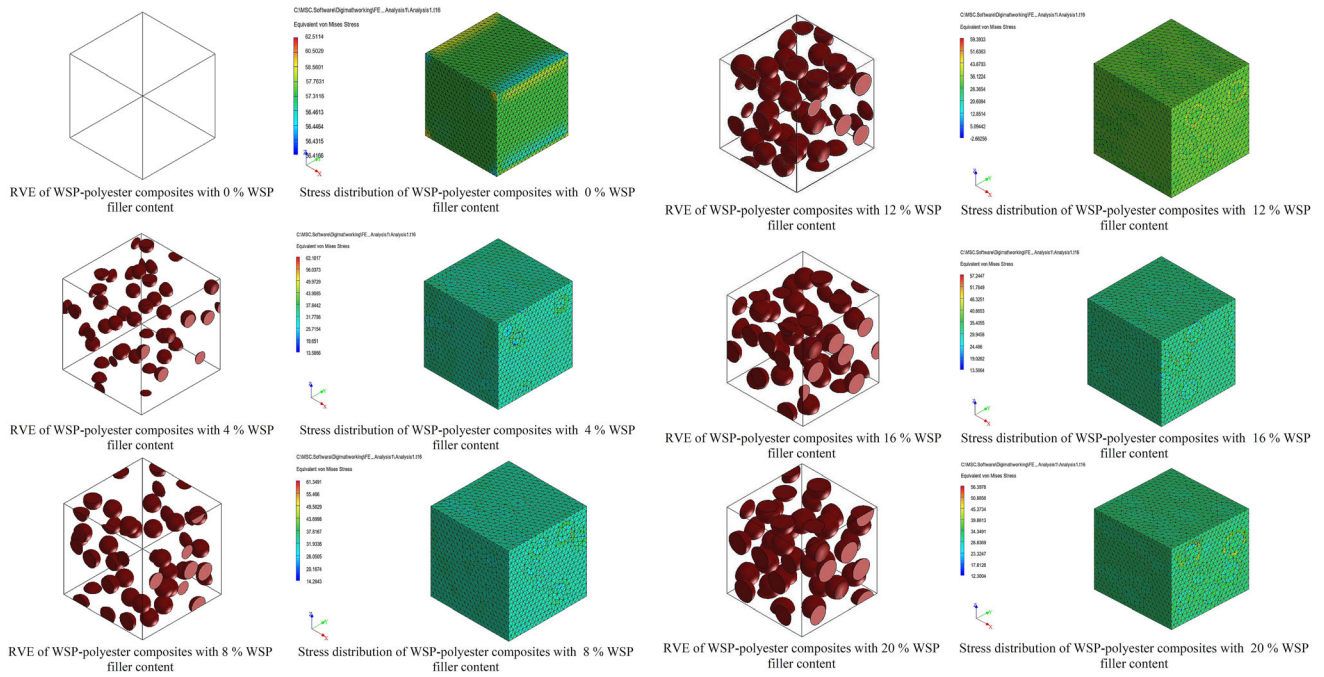


**Fig. 8** RVE and stress distribution of WSP–polyester composites with 0, 4, 8, 12, 16 and 20 wt.% of WSP

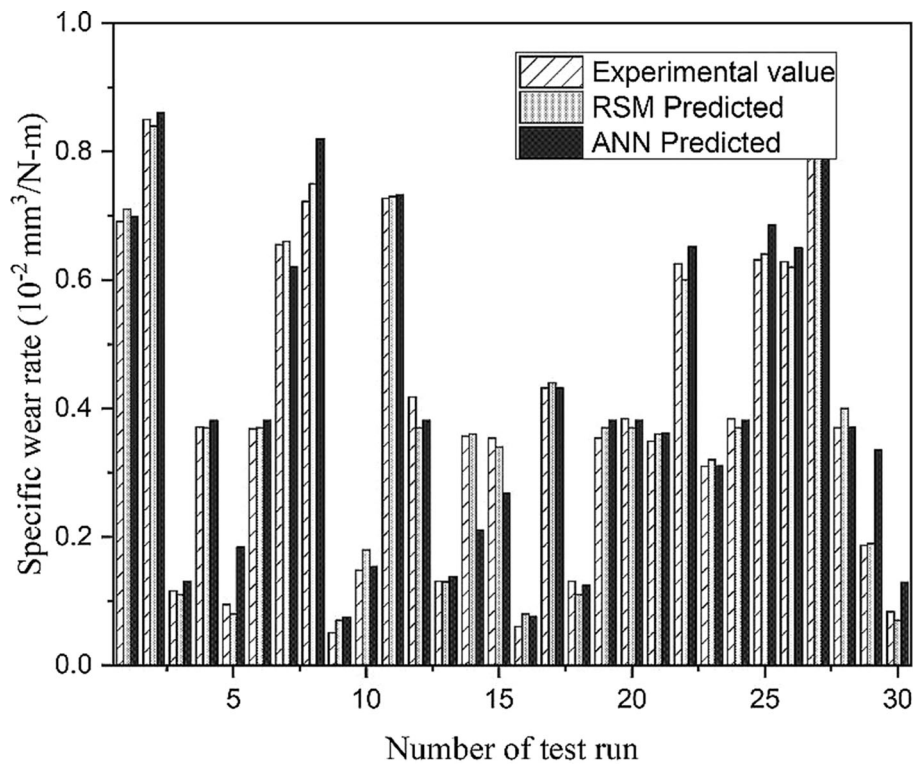


**Fig. 9** Comparison between RSM, ANN predicted and experimental result of SWR for WSP–polyester composites

by Digimat FE and the color contour presents the stress levels at different phases of the composite (Ref 26). The highest stress concentration of 62.5 MPa is observed for the composite sample with 0 wt.% of WSP filler. As the WSP filler loading increases up to 20 wt.%, the tensile strength of the composite decreases by about 24% compared to neat polyester. At higher

filler loading, composite shows lower stress level than that with a lower particle volume fraction when applied to the same strain rate. So material fails easily at higher filler content leads to a reduction in tensile strength of the composites. The SEM image of WSP–polyester composite with 12 wt.% filler content after tensile testing is shown in Fig. 6(a). When filler content is



**Table 2 ANOVA table for specific wear rate (before elimination)**

Source	Sum of squares	df	Mean square	F value	P value
Model	0.0002	14	0.0000	185.78	< 0.0001
A-Sliding velocity ( $V_s$ )	6.535E-06	1	6.535E-06	97.73	< 0.0001
B-Sliding distance ( $D$ )	1.309E-06	1	1.309E-06	19.58	0.0005
C-Normal load ( $F_n$ )	1.089E-11	1	1.089E-11	0.0002	0.9900
D-Filler content ( $f_s$ )	0.0002	1	0.0002	2441.37	< 0.0001
AB	4.536E-07	1	4.536E-07	6.78	0.0199
AC	1.823E-10	1	1.823E-10	0.0027	0.9591
AD	7.543E-07	1	7.543E-07	11.28	0.0043
BC	5.402E-09	1	5.402E-09	0.0808	0.7801
BD	2.223E-07	1	2.223E-07	3.32	0.0882
CD	1.014E-07	1	1.014E-07	1.52	0.2370
$A^2$	2.129E-08	1	2.129E-08	0.3184	0.5809
$B^2$	1.092E-12	1	1.092E-12	0.0000	0.9968
$C^2$	2.068E-08	1	2.068E-08	0.3093	0.5863
$D^2$	4.476E-07	1	4.476E-07	6.69	0.0206
Residual	1.003E-06	15	6.687E-08		
Lack of fit	7.653E-07	10	7.653E-08	1.61	0.3124
Pure error	2.377E-07	5	4.754E-08	185.78	
Cor total	0.0002	29		97.73	
Standard deviation = 0.0003			$R^2 = 0.9943$		
Mean = 0.0040			Adjusted $R^2 = 0.9989$		
Coefficient of variation = 6.53			Predicted $R^2 = 0.9677$		
Adequate precision = 43.5154					

**Table 3 ANOVA table for specific wear rate (after elimination)**

Source	Sum of squares	df	Mean square	F value	P value
Model	0.0002	8	0.0000	360.83	< 0.0001
A-Sliding velocity ( $V_s$ )	6.535E-06	1	6.535E-06	108.63	< 0.0001
B-Sliding distance ( $D$ )	1.309E-06	1	1.309E-06	21.76	< 0.0001
C-Normal load	1.089E-11	1	1.089E-11	0.0002	< 0.0001
D-Filler content	0.0002	1	0.0002	2713.66	< 0.0001
AB	4.536E-07	1	4.536E-07	7.54	0.0121
AD	7.543E-07	1	7.543E-07	12.54	0.0019
CD	1.014E-07	1	1.014E-07	1.69	0.0012
$D^2$	1.252E-06	1	1.252E-06	20.82	0.0002
Residual	1.263E-06	21	6.016E-08		
Lack of fit	1.026E-06	16	6.410E-08	1.35	0.3964
Pure error	2.377E-07	5	4.754E-08		
Cor total	0.0002	29			
Standard deviation = 0.0002			$R^2 = 0.9982$		
Mean = 0.0040			Adjusted $R^2 = 0.9900$		
Coefficient of variation = 6.59			Predicted $R^2 = 0.9811$		
Adequate precision = 59.0050					

increased in the composite, the ductility of material reduces and brittleness increases simultaneously as shown in Fig. 6(a) due to which tensile strength of the composite decreases. Similar type of behavior is also observed by Nitin and Singh during their study on the tensile strength analysis of WSP-epoxy composite (Ref 27).

### 3.3 Dry Sliding Wear Test Result

**3.3.1 RSM Analysis.** In this investigation, face-centered central composite design (FCCCD) which belongs to the response surface methodology (RSM) part set is used for the design of experiments (DoE). The experimental runs of

FCCCD consists total of 16 factorial points (a full factorial design with all combinations of the factors at the two levels). Out of these 16 factorial points, eight belongs to axial points, six-star points and two central points (Ref 28). Total 30 test runs have been carried out by maintaining the input parameters at designed levels. Each experimental test is performed in triplicate and the average value of results is considered as specific wear rate. The response, that is, the specific wear rate of each experiment is presented in Fig. 9. The analysis of the goodness of fit of the designed model is very much required for the examination of the data. Therefore, in this study, analysis of variance (ANOVA) is carried out on the wear responses of the

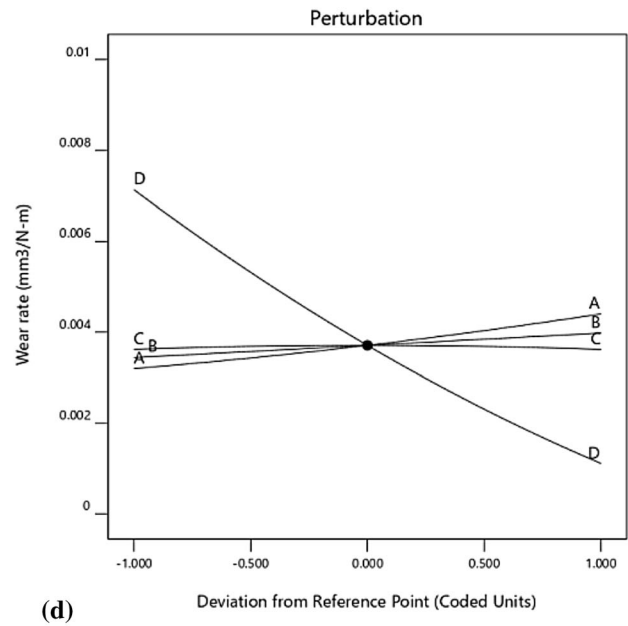
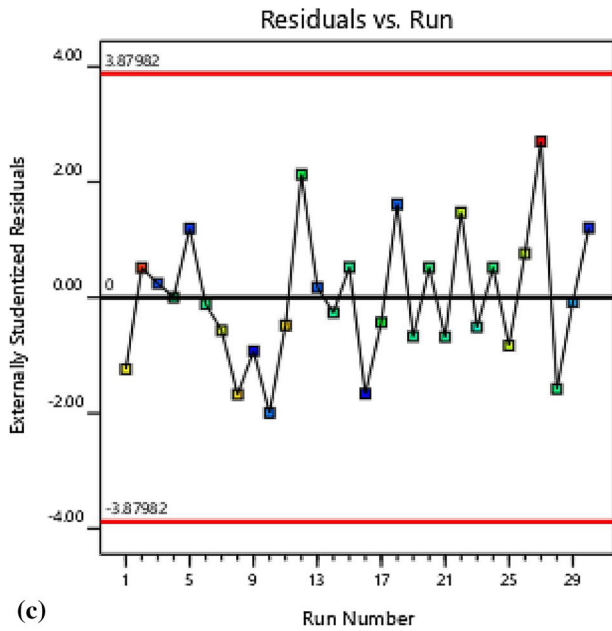
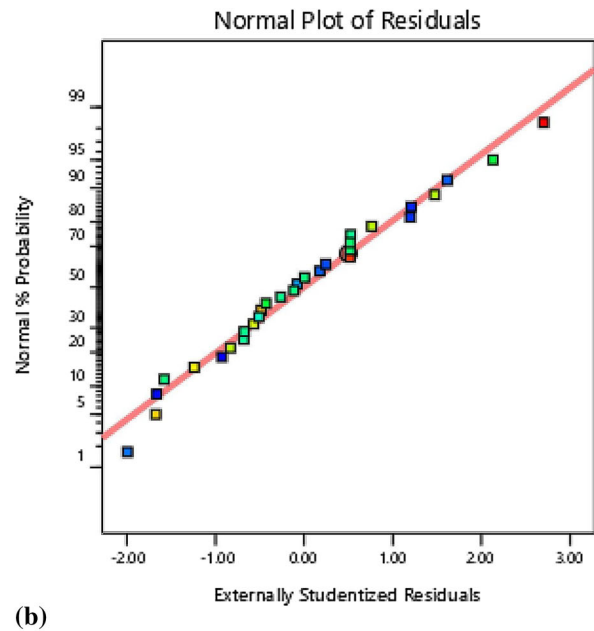
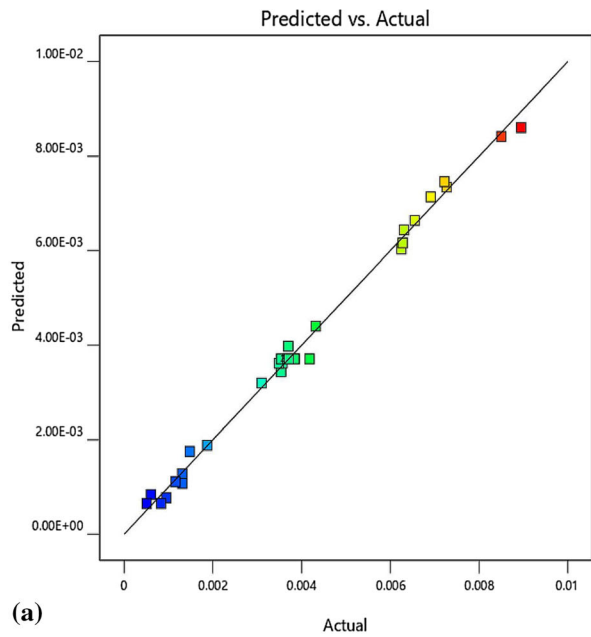


**Fig. 10** (a) Predicted versus actual plot of WSP–polyester composite. (b) Normal probability plot of WSP–polyester composite, (c) Residual plot of WSP–polyester composite, (d) Perturbation Plot of WSP–polyester composite

composites to analyze the adequacy of fit of the model.

**3.3.2 Analysis of Variance and Fitting Regression Model.** The fit summary of the sliding wear behavior of the WSP–polyester composites is conducted by response surface methodology (RSM), which indicates that the designed quadratic model is statically significant due to the higher value of adjusted  $R^2$  (0.9943). The dry sliding wear test results of the quadratic model in the form of ANOVA are illustrated in Table 2. ANOVA Table 2 shows that the associated p value for the quadratic model is smaller than 0.05 (i.e., 95% confidence, or  $\alpha = 0.05$ ), which indicates that the model is granted to be

statically significant. The value of the coefficient of determination ( $R^2$ ) is equal to 0.9943, which indicates that the response model confirms 99.43% of the total variation. The difference between  $R^2$  (0.9943) and adjusted  $R^2$  (0.9989) value is very less, which shows that the capacity of the quadratic model has been utilized effectively. As the value of both  $R^2$  and adjusted  $R^2$  for WSP–polyester composites is greater than 0.95, this confirms that the regression model presents an effective relation between independent process parameters and wear responses. For lack of fit, the associated p value should be greater than 0.05 because it shows any term left out of model is not

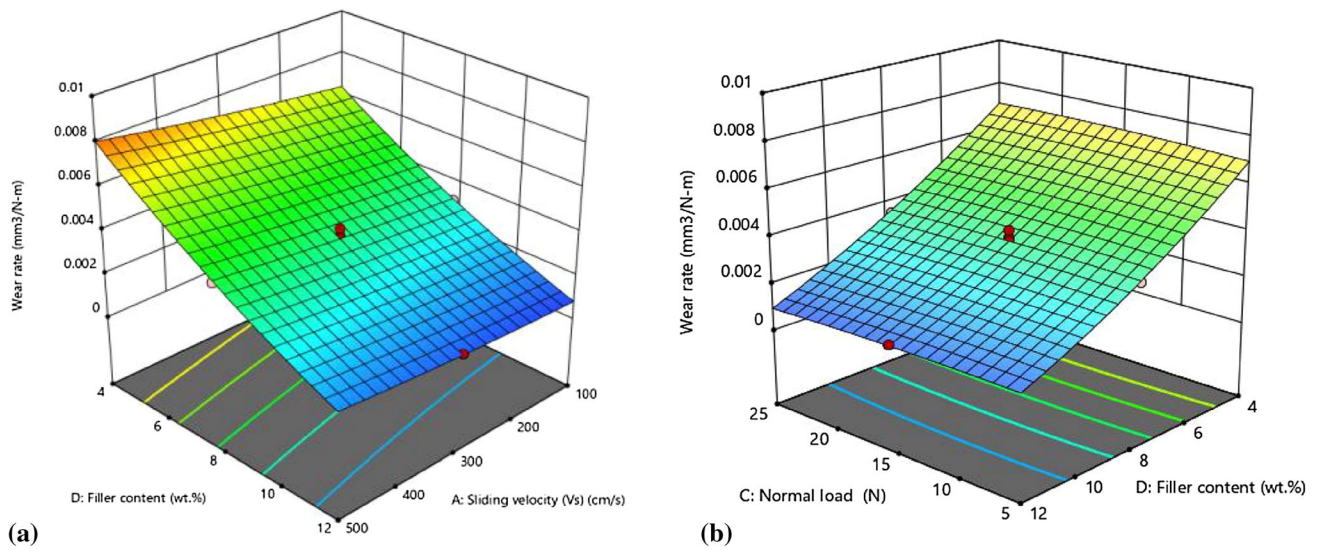


**Fig. 11** (a) Surface plot effect of filler content and sliding velocity on specific wear rate of WSP–polyester composite (b) Surface plot effect of filler content and normal load on the specific wear rate of WSP–polyester composite

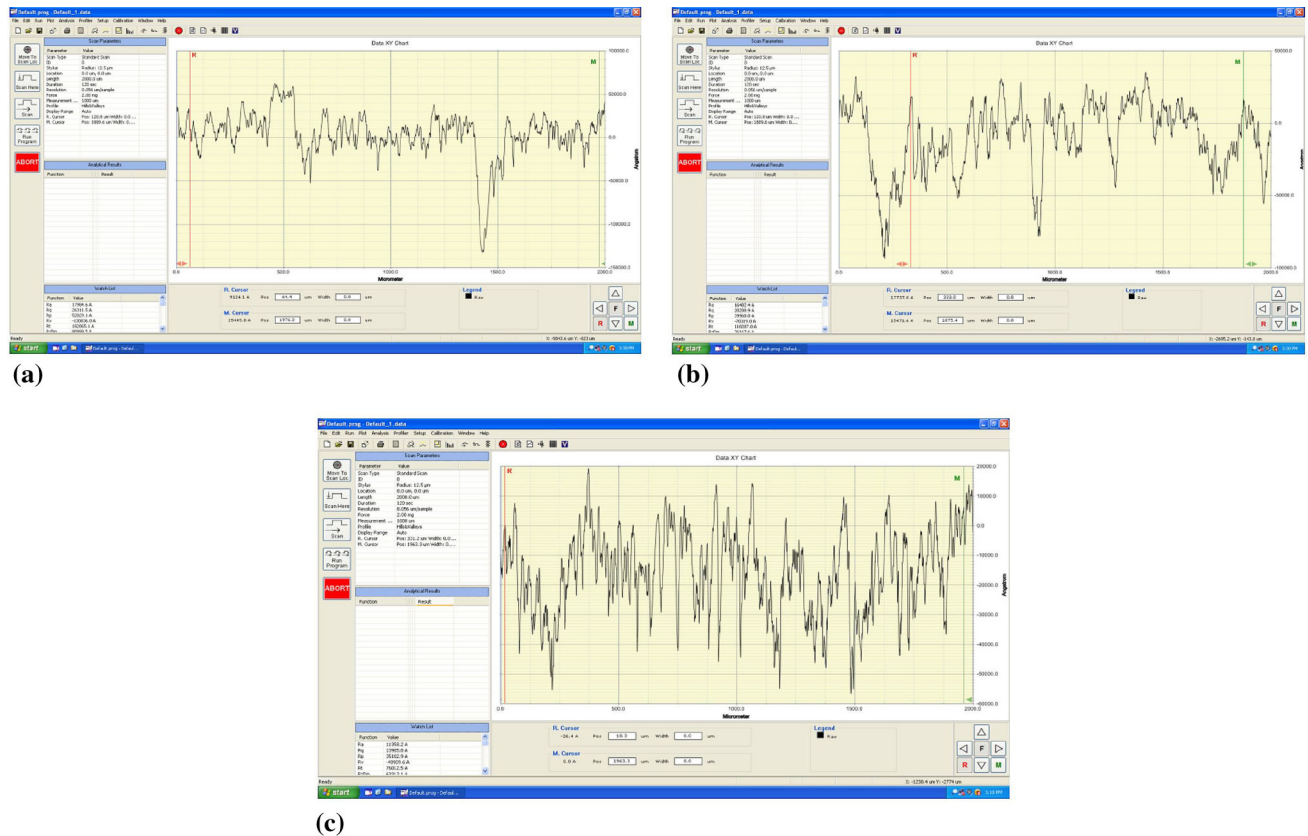


**Fig. 12** Surface roughness plot of WSP–polyester composites at (a) 4 wt.% , 500 cm s<sup>-1</sup>, 500 m, 5 N (b) 8 wt.% , 300 cm s<sup>-1</sup>, 1500 m, 25 N (c) 12 wt.% , 500 cm s<sup>-1</sup>, 500 m, 25 N

significant. The lack of fit p value for the regression model of WSP–polyester composite is 0.3124, which indicates that lack of fit is not significant so the designed model fits outstandingly. Further from the ANOVA Table 2, it could be observed that the factor sliding velocity ( $V_s$ ), filler content ( $f$ ), sliding distance ( $D$ ), interaction between filler content ( $f$ ) and sliding velocity

( $V_s$ ), the second-order term of factor filler content ( $f$ ) significantly affect the specific wear rate ( $W_s$ ) of the composites. The nonsignificant terms have been neglected by backward elimination so that the regression model can fit the wear rate ( $W_s$ ) effectively. The ANOVA table for the reduced quadratic model is presented in Table 3. The values of  $R^2$  (0.9982) and adjusted

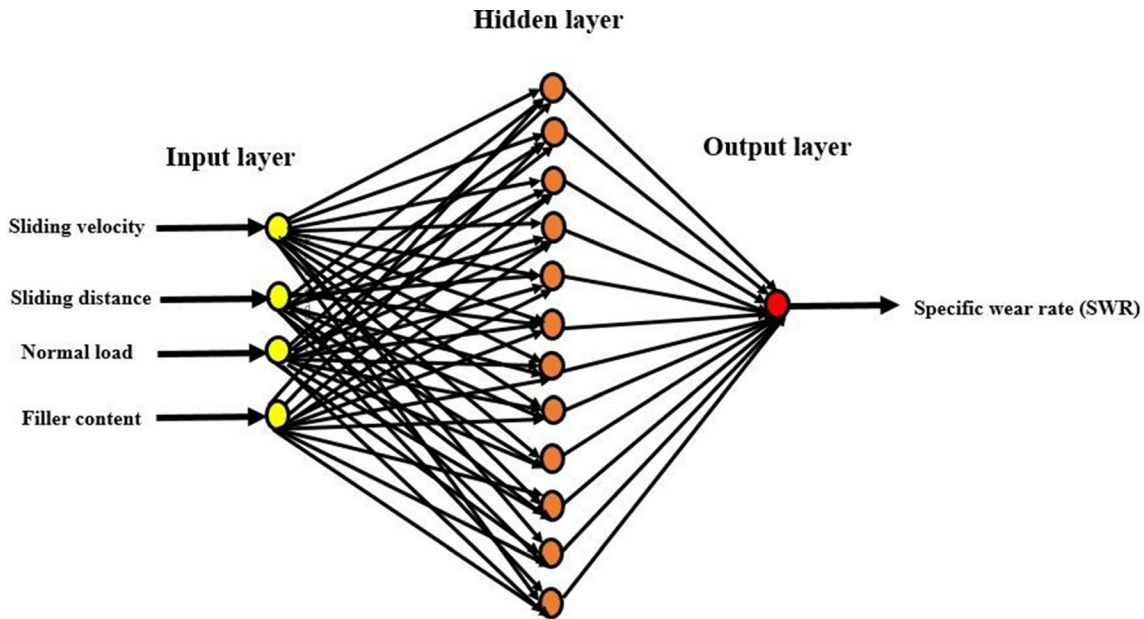


**Fig. 13** Constructed ANN model for prediction of specific wear rate

$R^2$  (0.9999) obtained from Table 3 indicates that the model is significant whereas the lack of fit (0.3964) is not significant. From the predicted versus actual plot shown in Fig. 10(a), it can be observed that the predicted wear rates of the composites are in good concurrence with the actual results. The normal plot residual for the specific wear rate of the composites is presented in Fig. 10(b). The normal plot of residuals closely falls into a straight line, which indicates that the errors are normally distributed. The graph plotted by residuals vs run is used to evaluate the independence of the data. The residual plot shown in Fig. 10(c) reveals that the graph does not take any shape of the predictable pattern because all the runs fall between range levels  $-4$  to  $4$ . This confirms the significance of ANOVA assumptions. The impact of all the factors on a single plot can be compared by perturbation plot. A perturbation plot is used to analyze the influence of all the factors on the specific wear rate at the center point, which is shown in Fig. 10(d). It can be observed from the perturbation plot that the specific wear rate, among all the factors, is predominantly affected by the concentration of the filler content in the WSP–polyester composites.

The final response equation to evaluate specific wear rate ( $W_s$ ) of the composites after eradicating the nonsignificant terms is mentioned below:

$$\begin{aligned}
 W_s = & 0.009582 + 3.92122E - 06V_s + 1.71024E - 08D \\
 & + 0.000016F_n - 0.001059f + 8.41875E \\
 & - 10V_sD - 2.71406E - 07V_s f - 1.99062E - 06F_n f \\
 & + 0.000026f
 \end{aligned}
 \tag{Eq 7}$$

The effect of filler content and sliding velocity on the specific wear rate of the WSP–polyester composites is shown in Fig. 11(a). Figure 11(a) shows that the specific wear rate of WSP–polyester composites decreases with the addition of filler content irrespective of sliding velocity. The shape of walnut shell powder forms an effective interlock with the matrix material. Due to which a transfer film is formed on the surface

of counterface, which behaves like a protective barrier to prevent large-scale fragmentation of polyester resin and prevents removal of material at higher filler loading. Also as WSP content increases in the composite, lignin concentration also increases and subsequently carbon content also increases as seen in the EDS analysis (12 wt.% WSP–polyester composite) shown in Fig. 3(b). Due to this, the bulk effective hardness of the composite increases. This may be another reason behind this abatement in SWR at higher filler loading. Doddamani et al. also reported decrease in specific wear rate of WSP–epoxy composite with increase in filler content (Ref 29). The effect of normal load and filler concentration on the specific wear rate of the composites is presented in Fig. 11(b). The wear is primarily generated at the contact surface of the pin and sliding disk. The increase in normal load results in a simultaneous rise in frictional thrust causing occurrence of debonding between filler and matrix. Also at higher loads, irregular shaped walnut shell particles with sharp edges penetrate in to the surface of the disk. This leads to an increase in the wear rate of the composite material at higher loads. The surface roughness of WSP–polyester composites is measured by profile meter and the Ra value is presented in Fig. 12. Figure 12(a), (b), and (c) shows the surface roughness pattern of the composites at (a) 4 wt.% ,  $500 \text{ cm s}^{-1}$ , 500 m, 5 N (b) 8 wt.% ,  $300 \text{ cm s}^{-1}$ , 1500 m, 25 N (c) 12 wt.% ,  $500 \text{ cm s}^{-1}$ , 500 m, 25 N respectively. The surface roughness value of 4 wt.% composite is found to be 1.79 Ra under 5 N, whereas the surface roughness of 8 and 12 wt.% composite is 1.6 and 1.1 Ra under 25 N load, respectively. The roughness of the composites is decreasing with increase in filler content even at higher load which signals that SWR is not only affected by normal load but also influenced significantly by the filler content.

**3.3.3 Prediction using Artificial Neural Network (ANN).** **3.3.3.1 Network Testing and Training.** From the above discussion, it is concluded that dry sliding wear behavior of the WSP–polyester composites depends upon many factors and the impact of these factors should be analyzed carefully

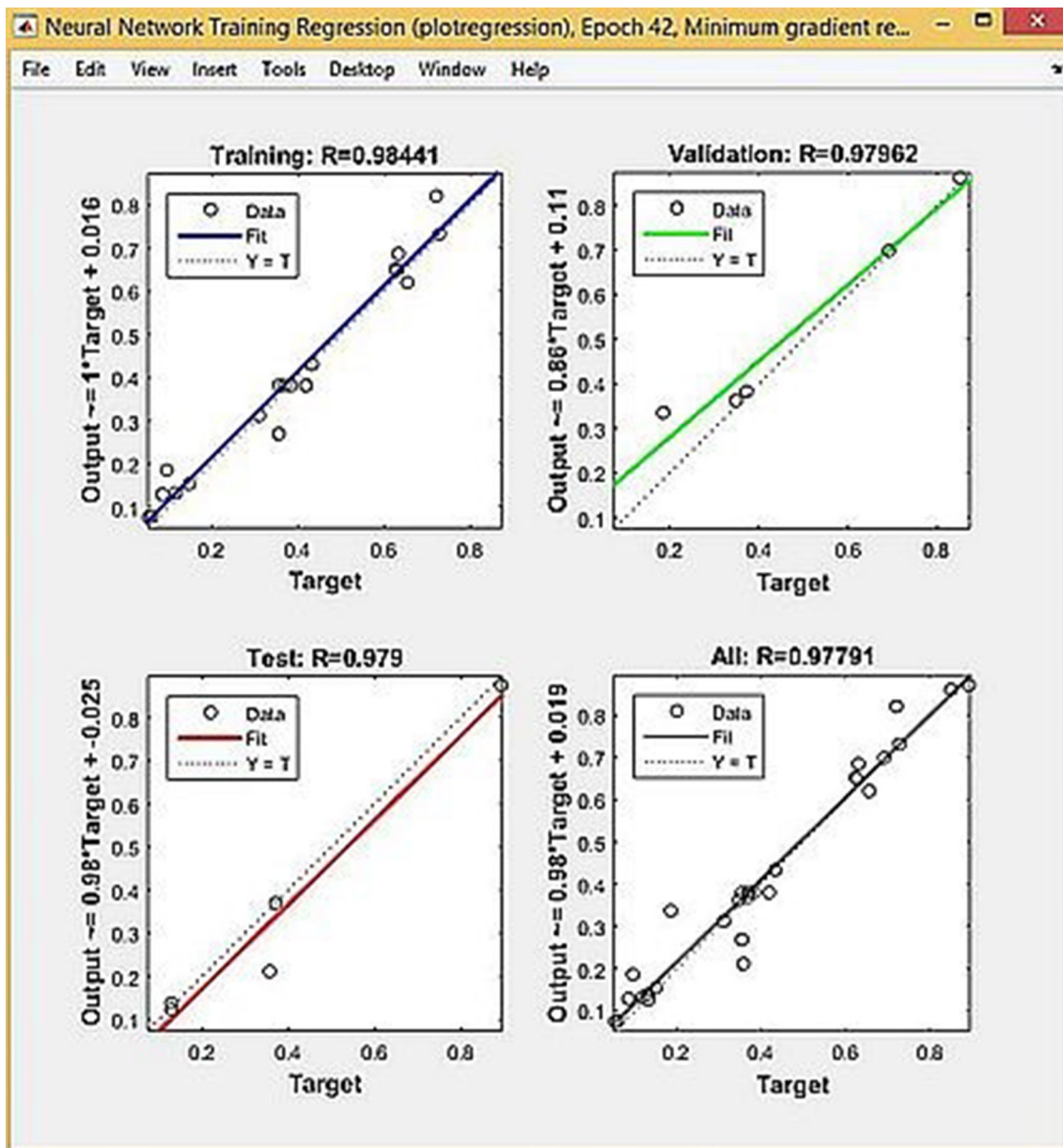


**Fig.14** Coefficient of Determination obtained by training a network

beyond the test domain used in this investigation. Artificial neural network (ANN) is a technique, which could be used to simulate, analyze and predict the output for wide range of input. Therefore, in the present work, artificial neural network (ANN) is used to validate the model obtained from response surface methodology and predict the output with combination of different input parameters. A neural network is created based on the experimental data in three steps such as training, testing and prediction. This network can be used to solve complex and nonlinear problems because it works like human brain, which means it can learn directly from the supplied data without providing any formula.

**3.3.3.2 Preparation of the Specific Wear Rate Database.** The specific wear rate of WSP–polyester composite with different filler concentration (4, 8 and 12 wt.%) is measured by pin-on-disk machine. Total 30 experiments have been conducted according to design of experiments (DoE) prepared by

face-centered central composite design (FCCCD). The result obtained from the experiments is used as database for training the network.

**3.3.3.3 Training the Network.** A neural network consists of several cross-linked simple processing unit called neurons. A neural network has three different layers connected in series such as (i) input layer (ii) hidden layer (iii) output layer. Input layer receives the information while hidden layer carries out-processing of this information. Finally, the result is exported by output layer. In this analysis, a three-layer ANN model is constructed as shown in Fig. 13 which consists four neurons the input layer, which represent sliding velocity, sliding distance, normal load, and filler content, whereas the output layer has one neuron as specific wear rate. But, the number of neuron in the hidden layer is chosen by hit and trial method, and is obtained 12. The results obtained from experiments are utilized to train the network. The input variables are normalized so that all the

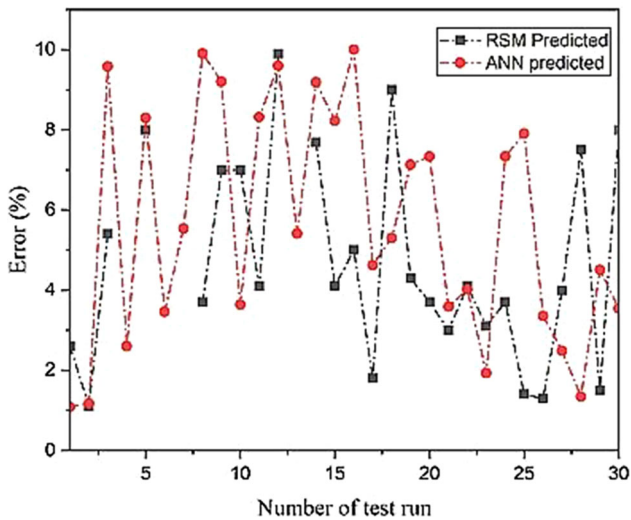


Fig. 15 Error (%) of RSM and ANN predicted SWR with experimental result

values fall in same range 0-1. Total 30 numbers of experiments are used for training the network. Several ANN structures are tested with different numbers of neurons present in the hidden layer. But the optimized network is obtained with 12 neurons in the hidden layer. One network is selected for the training of input–output data based on least error criterion. The network is chosen for prediction when coefficient of determination reached  $R = 0.97791$  as shown in Fig. 14.

**3.3.3.4 Testing of the Neural Network.** The testing aims to evaluate the network performance. The framed neural network is trained by considering the input database obtained from sliding wear tests. Then it is simulated to predict the same 30 numbers experiments used in response surface methodology. The comparison between the ANN, RSM predicted specific wear rate of WSP–polyester composites with experimental result is presented in Fig. 13.

**3.3.4 Predicting the Specific Wear Rate of the WSP–Polyester Composites for a New Domain Data Set.** Figure 9 shows that the designed neural network predicts the specific wear rate of the composites very similar to RSM and experimental results and the corresponding errors lie within a range of 0–10 percent as shown in Fig. 15. Therefore, this well-trained neural network can be very useful to study the effect of input parameters with new domain of data set on the specific wear rate of the composites even beyond the experimental range.

**3.3.4.1 Effect of Sliding Velocity on the Specific Wear Rate of the Composites.** Figure 16(a) shows that the specific wear rate of composites increase monotonically with the sliding velocity. When sliding velocity increases, more heat is generated at the contact surface of the composite pin and the disk. Due to this, the temperature at the surface of the composite rises and this increase in temperature not only damages the mechanical properties but also weakens the bonding between the polymer and filler (Ref 30). In the year 2012, similar kind of result is observed by Rout and Satapathy from their investigation on rice husk-filled epoxy composites (Ref 1). Padhi et al. found that specific wear rate of blast furnace slag–epoxy composite increases with increase in sliding velocity up to certain limit and beyond that it decreases

marginally (Ref 17). More recently, investigation conducted by Nayak and Satapathy on marble dust-filled polyester composites showed similar types of findings in their study (Ref 31). Omrani et al. have also reported poor wear performance for jute/pp composites at higher sliding speed (Ref 30).

**3.3.4.2 Effect of Filler Content on the Specific Wear Rate of the Composites.** The effect of filler content on the specific wear rate of the composites is shown in Fig. 16(b). Figure 16(b) shows that the specific wear rate of polyester resin decreases with addition of WSP filler content at any range of sliding velocity. As shown in Fig. 17(a), the microstructure of walnut shell consists of stone cells of high lignification, which are relatively short and isodiametric, whereas the thickness of secondary wall is varied and filled up with lumina and lignin (Ref 32). These cells are comprised of about 90% of shell volume, which provide high strength and stiffness to walnut shell in comparison with wood flour (Ref 33). Similar structural features can also be noticed in the SEM image 17 (b) of walnut shell powder. The maximum drop in the specific wear rate can be seen for WSP–polyester composites with 12 wt.% of filler content and this drop possibly occurs due to the presence of these harder walnut shell particles. Investigation carried out by Kranthi and Satapathy also found that inclusion of pine wood dust improves the wear resistance capacity of epoxy composites (Ref 4). Pashaei and Hosseinzadeh observed that wear volume loss of WSP-filled vinyl ester composites decreases with increase in WSP content (Ref 34). Similarly, the co-efficient of friction and wear resistance of the walnut shell powder, jute and phenolic binder composites are improved significantly when filler content increases from 0 to 5.6 wt.% and these materials can be used in eco-friendly brakes (Ref 35).

**3.3.4.3 Effect of Normal Load on the Specific Wear Rate of the Composites.** The variation in the specific wear rate of WSP–polyester composites with filler content at different normal load is shown in Fig. 16(c). During prediction, the sliding distance and sliding velocity value is kept constant. Figure 16(c) clearly illustrates that increase in normal load accelerates the material removal rate from the surface of the composite. This material removal mechanism could be explained by Archard equation which states that increment in specific wear rate is directly proportional to the applied load (Ref 36). When normal load increases, the contact surface between pin and disk increases which leads to enhancement of temperature and stress level in the composite (Ref 37). This increase in temperature on the surface of the composite paves way to the debonding between filler and matrix due to which pulling out of WSP takes place. This pulling out of particles creates small craters which in turn increase SWR value of the composites. Pattnaik et al. in his investigation clearly described the relation between normal load and specific wear rate of the composites along this line (Ref 38).

**3.3.4.4 Effect of Sliding Distance on the Specific Wear Rate of the Composites.** The variation in the specific wear rate as a function of sliding distance is presented in Fig. 16(d). SWR of the composites is predicted by the constructed ANN model by considering constant normal load and sliding distance. The SWR remains high up to 2500m for all the composites irrespective of filler content and beyond that it starts reducing slightly. At the beginning, the abrasive particles of the sand paper easily penetrate in to the composite due to which more removal of material takes place. But at longer sliding distance, sand paper becomes smooth due to which size of abrasive particles decrease leads to lesser penetration into the composite

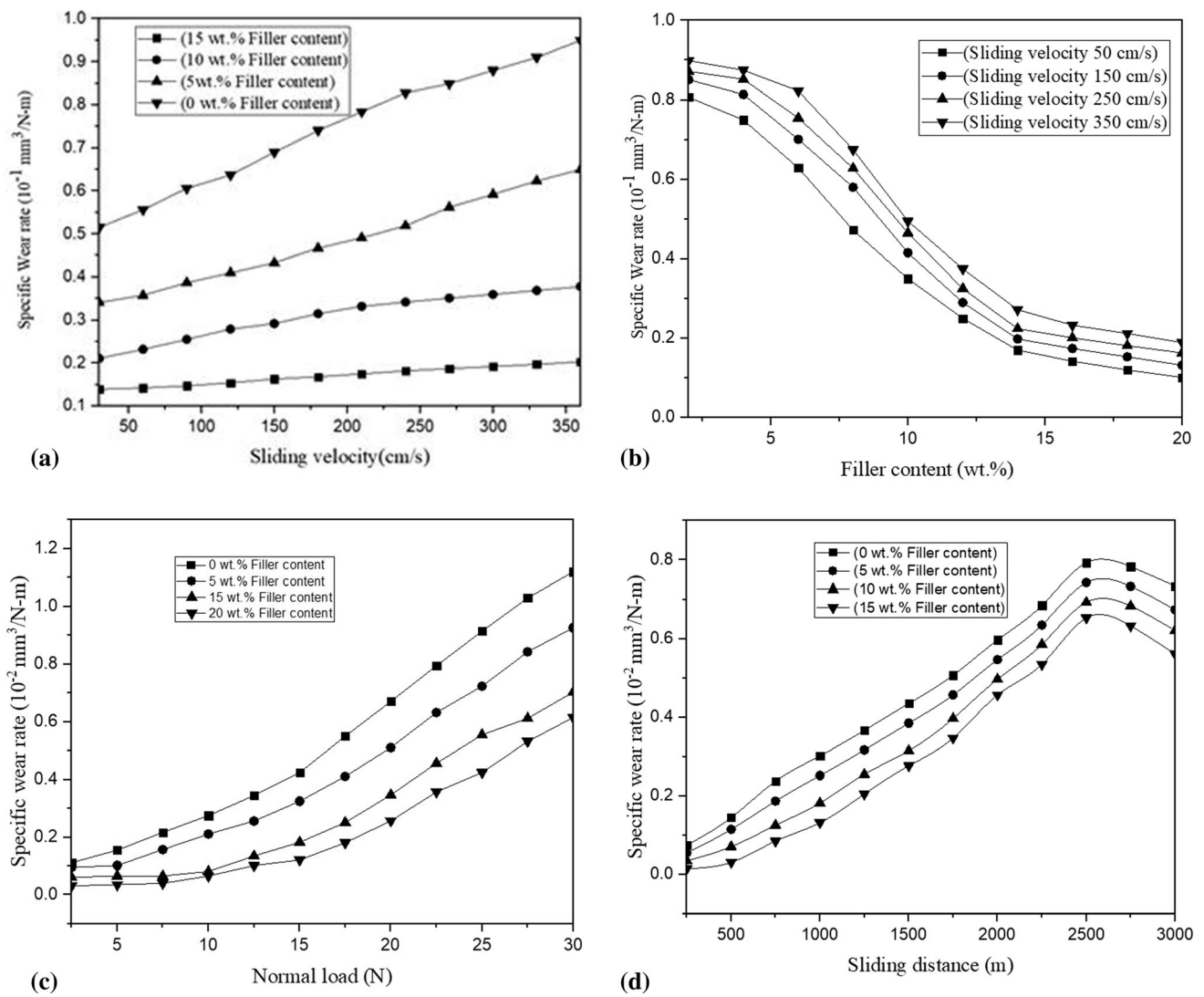


**Figure 16** (a) Variation of specific wear rate of WSP-polyester composites with sliding velocity for different filler content. (b) Variation of specific wear rate of WSP-polyester composites with filler content for different sliding velocity. (c) Variation of specific wear rate of WSP-polyester composites with normal load for different filler content. (d) Variation of specific wear rate of WSP-polyester composites with sliding distance for different filler content

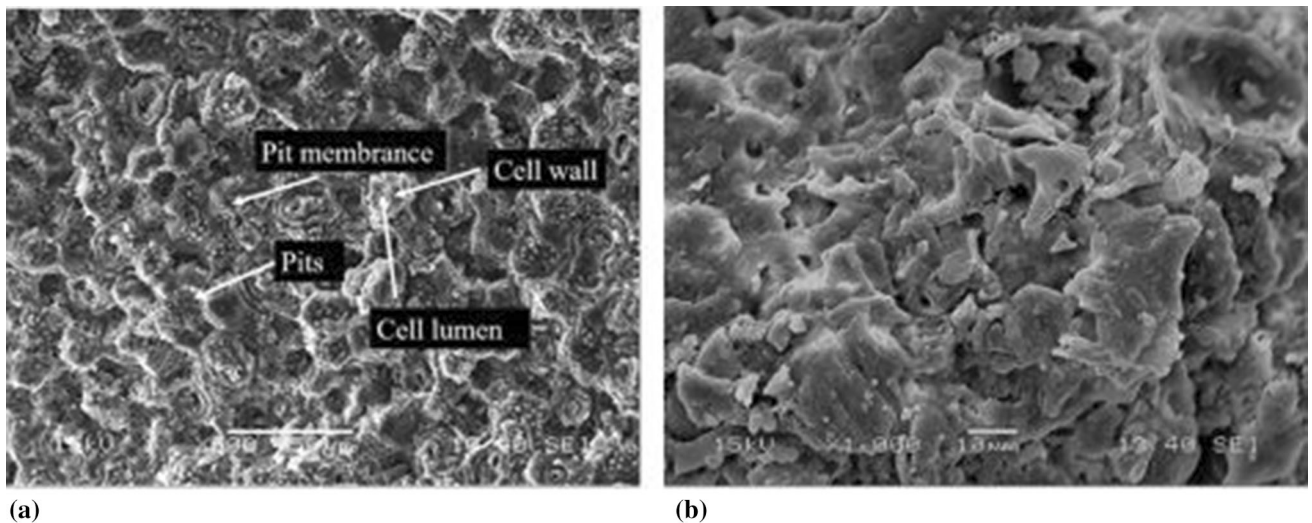


**Fig. 17** SEM image of (a) walnut shell and (b) walnut shell powder

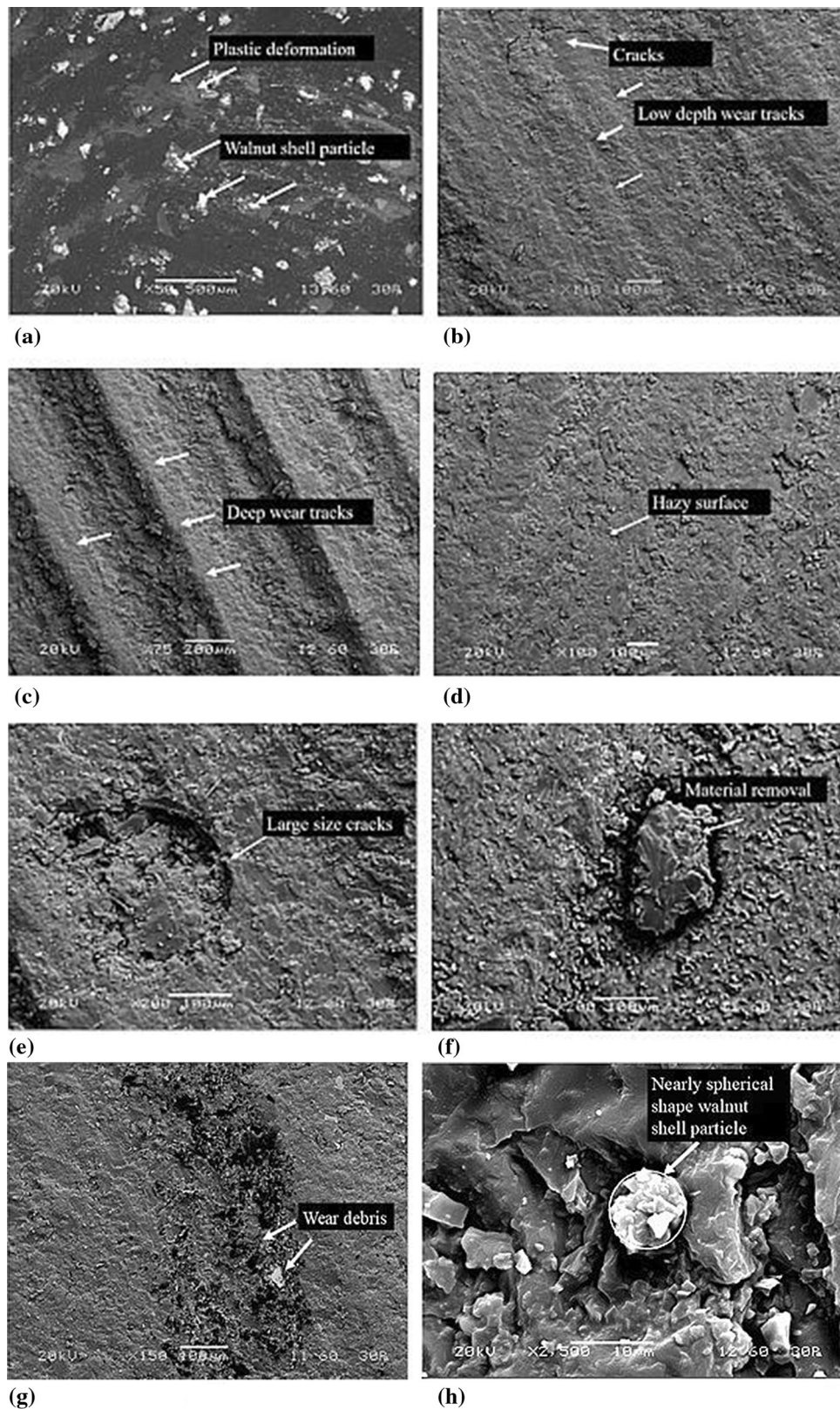


**Fig. 18** SEM micrographs of worn surface for WSP–polyester composites at different test condition (a) 12 wt.%, 500 cm s<sup>-1</sup>, 500 m, 25 N (b) 8 wt.% , 300 cm s<sup>-1</sup>, 1500 m, 25 N (c) 4 wt.% , 500 cm s<sup>-1</sup>, 500 m, 5 N (d) 4 wt.% , 100 cm s<sup>-1</sup>, 2500 m, 5 N (e) 4 wt.% , 300 cm s<sup>-1</sup>, 1500 m, 15 N (f) 4 wt.% , 100 cm s<sup>-1</sup>, 2500 m, 25 N (g) 8 wt.% , 300 cm s<sup>-1</sup>, 1500 m, 15 N (h) nearly spherical shape walnut shell particle



surface. Pradhan et al. found similar type of result during their investigation on the epoxy-lantana camara fiber composites (Ref 8).

**3.3.5 Morphology of Worn Samples.** The scanning electron micrographs of the composite worn surfaces are presented in Fig. 18(a), (b), (c), (d), (e), (f), and (g). Figure 18(a) shows micrograph of WSP–polyester composite containing 12 wt.% of filler content after testing at sliding velocity  $500\text{ cm s}^{-1}$ , sliding distance 500 m and 25 N load. From the SEM image, the uniform distribution of walnut shell particles is clearly visible. But even at 25 N load wear tracks cannot be observed clearly on the surface of the composites, which signals that composite at higher filler loading is capable of resisting the wear effectively even at higher applied load. Figure 18(b) shows SEM image of composite containing 8 wt.% of filler at sliding velocity  $300\text{ cm s}^{-1}$ , sliding distance 1500 m and 25 N load. Wear tracks with comparatively lower indentation could be identified which is created due to relative motion between composite and the countersurface of the rotating disk. Figure 18(c) is the SEM image of worn surface of the composites containing 4 wt.% of WSP content after sliding distance 500 m at  $500\text{ cm s}^{-1}$  velocity under 5N load. Figure 18(c) shows that deep wear tracks are present on the surface of the composites even when tested under lower load. This clearly shows that identification of wear track becomes very difficult with increase in filler content. The SEM image of composites with 4 wt.% filler content at velocity  $100\text{ cm s}^{-1}$  tested after 2500 m under 5 N is shown in Fig. 18(d). The surface is looking hazy and comparatively smoother. After being tested for long sliding distance, the sand paper becomes smoother and not able to penetrate more effectively in to composites due to which wear rate decreases with longer sliding distance. Figure 18(e) and (f) present the worn surface of composites at 4 wt.% ,  $300\text{ cm s}^{-1}$ , 1500 m, 15 N and 4 wt.% ,  $100\text{ cm s}^{-1}$ , 2500 m, 25 N, respectively. When load is increased, more heat is generated between the composites and countersurface, which makes the material softer. Due to which plastic deformation occurs and cracks are formed on the surface of the composites. When load is again increased from 15 to 25 N, this micro-fracture leads to the material removal from the surface of the composite as shown in Fig. 18(f). Figure 18(g) illustrates the SEM image image of worn surface of composite at 8 wt.%,  $300\text{ cm s}^{-1}$ , 1500 m, 15 N. The wear debris and plastic deformation are clearly identified on the surface. This may be occurring due to decrease in ductility of the composites as a result of higher filler content in the matrix body but it is difficult to find wear tracks (Ref 31).

## 4. Conclusions

This work shows that the walnut shell, despite being an agricultural waste, can be a source for a functional filler material. The reinforcing potential of the walnut shell powder is established by successfully fabricating polyester-based composites using it as the filler through the simple hand layup technique. It is found that the density, porosity, tensile strength, etc., of these composites depend on the filler loading. Dry sliding wear behavior of the composites is studied experimentally and the responses are analyzed using a novel statistical technique like response surface methodology. The analysis shows that the wear rate of the composites is largely dependent

on the walnut shell powder content. Its inclusion as a filler enhances the wear resistance capability of polyester resin under different dry sliding conditions. This work also proposes a prediction model based on artificial neural networks for estimating specific wear rates of composites with different filler concentrations and test conditions within and beyond the experimental domain.

## References

1. A. Rout and A. Satapathy, "Analysis of Dry Sliding Wear Behaviour of Rice Husk Filled Epoxy Composites Using Design Of Experiment and ANN," *Procedia Eng.*, 2012, **38**, p 1218–1232
2. N.F. Zaaba and H. Ismail, Thermoplastic/Natural Filler Composites: A Short Review, *J. Phys. Sci.*, 2019, **30**, p 81–99
3. K.H.K.A. Lakshumu Naidu and B. Sudarshan, Study on Mechanical Behavior of Groundnut Shell Fiber Reinforced Polymer Metal Matrix Composites A.Lakshumu, *Int. J. Eng. Res. Technol.*, 2013, **2(2)**, p 1–8
4. G. Kranthi and A. Satapathy, Evaluation and Prediction of Wear Response of Pine Wood Dust Filled Epoxy Composites Using Neural Computation, *Comput. Mater. Sci.*, 2010, **49(3)**, p 609–614
5. O.D. Samuel, S. Agbo and T.A. Adekanye, Study of Mechanical Behaviour of Coconut Shell Reinforced Polymer Matrix Composite, *J. Miner. Mater. Charact. Eng.*, 2012, **11(08)**, p 774–779
6. B. Dan-asabe, Thermo-Mechanical Characterization of Banana Particulate Reinforced PVC Composite as Piping Material, *J. King Saud Univ. Eng. Sci.*, 2018, **30(4)**, p 296–304
7. P. Pradhan, Polyester Composites Filled with Walnut Shell Powder: Preparation and Thermal Characterization, 2020, no. March, p 1–1
8. S. Pradhan and S. Kumar Acharya, "Study of Mechanical and Abrasive Wear Properties of Lantana Camara Particulate Reinforced Epoxy Composite," *Mater. Today Proc.*, 2019, p 1–5
9. H. Aireddy and S.C. Mishra, Tribological Behavior and Mechanical Properties of Bio-Waste Reinforced Polymer Matrix Composites, *J. Metall. Mater. Sci.*, 2011, **53(2)**, p 139–152
10. N. Ayrlimis, A. Kaymakci and F. Ozdemir, Physical, Mechanical, and Thermal Properties of Polypropylene Composites Filled with Walnut Shell Flour, *J. Ind. Eng. Chem.*, 2013, **19(3)**, p 908–914
11. A. Srinivasan and T. Viraraghavan, Removal of Oil by Walnut Shell Media, *Bioresour. Technol.*, 2008, **99(17)**, p 8217–8220
12. S. D. Lala, A. B. Deoghare and S. Chatterjee, Mechanical and Morphological Characterization of Walnut Shell Reinforced Epoxy Composite, *IOP Conf. Ser. Mater. Sci. Eng.*, 2018, vol. 377, no. 1
13. N.A. Sarsari, S. Pourmousa and A. Tajdini, Physical and Mechanical Properties of Walnut Shell Flour-Filled Thermoplastic Starch Composites, *BioResources*, 2016, **11(3)**, p 6968–6983
14. M. U. Obidiegwu, S. C. Nwanonyeni, I. O. Eze and I. C. Egbuna, The Effect of Walnut Shell Powder on the Properties of Polypropylene Filled Composite, 2014, vol. **02(1)**, p 22–29
15. Z. Zhang and K. Friedrich, Artificial Neural Networks Applied to Polymer Composites: A Review, 2003, vol. **63**, p 2029–2044
16. K. K. Ekka and S. R. Chauhan, "Study on the Sliding Wear Behaviour of Hybrid Aluminium Matrix Composites Using Taguchi Design and Neural Network, 2016, vol. **230**, no. 2, p 537–549
17. P.K. Padhi, A. Satapathy and A.M. Nakka, Processing, Characterization, and Wear Analysis of Short Glass Fiber-Reinforced Polypropylene Composites Filled with Blast Furnace Slag, *J. Thermoplast. Compos. Mater.*, 2015, **28(5)**, p 656–671
18. G. Satyanarayana, G. Swami and N.H. Babu, "Artificial Neural Network and Regression Modelling to Study the Effect of Reinforcement and Deformation on Volumetric Wear of Red Mud Nano Particle Reinforced Aluminium Matrix Composites Synthesized by Stir Casting", *Boletín la Soc. Española Cerámica y Vidr.*, 2017, **57(3)**, p 91–100
19. H. Pirayesh, A. Khazaeian and T. Tabarsa, The Potential for Using Walnut (*Juglans regia* L.) Shell as a Raw Material for Wood-Based Particleboard Manufacturing, *Compos. Part B Eng.*, 2012, **43(8)**, p 3276–3280
20. S. Ojha, R. Gujjala and S. Acharya, Effect of Filler Loading on Mechanical and Tribological Properties of Wood Apple Shell Reinforced Epoxy Composite, *Adv. Mater. Sci.*, 2013, **2014**, p 1–9

21. K. Gajalakshmi, N. Senthilkumar and B. Prabu, Multi-Response Optimization of Dry Sliding Wear Parameters of AA6026 Using Hybrid Gray Relational Analysis Coupled with Response Surface Method, *Meas. Control (United Kingdom)*, 2019, **52**, p 540–553
22. D. K. Prajapati and M. Tiwari, Use of Artificial Neural Network (ANN) to Determining Surface Parameters, Friction and Wear during Pin-on-Disc Tribotesting, 2017, vol. **739**, p 87–95
23. M. Hayajneh, A. M. Hassan, A. Alrashdan and A. T. Mayyas, Prediction of Tribological Behavior of Aluminum–Copper Based Composite Using Artificial Neural Network, 2009, vol. **470**, p 584–588
24. Y. Chen and X. Cheng, Research on Characteristic of Walnut Shell High Boiling Solvent Lignin by Chemical Analysis, IR and NMR, *2011 International Conference on Remote Sensing, Environmental and Transportation Engineering RSETE 2011 Proc.*, 2011, p 8446–8449
25. P.A.-M.P.C.B.H.R.F.C.K. Bhagat, S. Biswas and J. Dehury, Polyvinyl Alcohol-Modified Pithcellobium Clypearia Benth Herbal Residue FiberPolypropylene Composites, *Polym. Compos.*, 2016, **37**(1), p 915–924
26. S. Goudar, R.K. Jain and D. Das, Physico-Mechanical Properties of Tamarind Pod Shell-Based Composite, *Polym. Compos.*, 2020, **41**(2), p 505–521
27. S. Nitin and V.K. Singh, Mechanical Behaviour of Walnut Reinforced Composite, *J. Mater. Environ. Sci.*, 2013, **4**(2), p 233–238
28. A. Purohit and A. Satapathy, Processing, Characterization, and Parametric Analysis of Erosion Behavior of Epoxy-LD Sludge Composites Using Taguchi Technique and Response Surface Method, *Polym. Compos.*, 2018, **39**, p E2283–E2297
29. J. Jain, S. Jain and S. Sinha, Characterization and Thermal Kinetic Analysis of Pineapple Leaf Fibers and Their Reinforcement in Epoxy, *J. Elastomers Plast.*, 2019, **51**(3), p 224–243
30. E. Omrani, P.L. Menezes and P.K. Rohatgi, Engineering Science and Technology, an International Journal State of the Art on Tribological Behavior of Polymer Matrix Composites Reinforced with Natural Fibers in the Green Materials World, *Eng. Sci. Technol. an Int. J.*, 2016, **19**(2), p 717–736
31. S. K. Nayak and A. Satapathy, Wear Analysis of Waste Marble Dust-Filled Polymer Composites with an Integrated Approach Based on Design of Experiments and Neural Computation, 2019, vol. 0, no. 0, p 1–11
32. J.A. Pereira, I. Oliveira, A. Sousa, I.C.F.R. Ferreira, A. Bento and L. Estevinho, Bioactive Properties and Chemical Composition of Six Walnut (*Juglans regia* L.) Cultivars, *Food Chem. Toxicol.*, 2008, **46**(6), p 2103–2111
33. R. Khantwal, G. Gupta and R. S. Negi, Walnut Shell Reinforced Composite: A Review, 2016, vol. **7**(5), p 179–189
34. S. Pashaei and S. Hosseinzadeh, Sliding Wear Behaviour of Walnut Shell Powder Filled Vinyl Ester/ WSP Green Composites, *Iran. Chem. Commun.*, 2017, **5**, p 138–146
35. S. Qi *et al.*, Effects of Walnut Shells on Friction and Wear Performance of Eco-Friendly Brake Friction Composites, *Proc. Inst. Mech. Eng. Part J J. Eng. Tribol.*, 2014, vol. **228**(5), p 511–520
36. L. Choudhary, P. Chhotani and J. Menghani, Study on Wear Behaviour on Hardfacing Alloy, *Trans. Indian Inst. Met.*, 2019, **72**(9), p 2465–2475
37. V. Kavimani, K. S. Prakash and T. Thankachan, Surface Characterization and Specific Wear Rate Prediction of r-GO/AZ31 Composite Under Dry Sliding Wear Condition, 2017, **6**, p 143–153
38. A. Patnaik, A. Satapathy, S. Biswas and B.K. Satapathy, A Study on a Possible Correlation Between Thermal Conductivity and Wear Resistance of Particulate Filled Polymer Composites, *Mater. Des.*, 2010, **31**(2), p 837–849

**Publisher's Note** Springer Nature remains neutral with regard to jurisdictional claims in published maps and institutional affiliations.